Hindawi
Journal of Chemistry
Volume 2020, Article ID 6645351, 16 pages
https://doi.org/10.1155/2020/6645351

Research Article

Chitin Hydrogels Prepared at Various Lithium Chloride/*N*,*N*-Dimethylacetamide Solutions by Water Vapor-Induced Phase Inversion

Khoa Dang Nguyen [1] **and Takaomi Kobayashi** [2]

[1]*Faculty of Technology, Van Lang University, 45 Nguyen Khac Nhu Street, Co Giang Ward, District 1, Ho Chi Minh City 71013, Vietnam*
[2]*Department of Science of Technology Innovation, Nagaoka University of Technology, 1603-1 Kamitomioka, Nagaoka, Niigata 940-2188, Japan*

Correspondence should be addressed to Khoa Dang Nguyen; khoa.nd@vlu.edu.vn

Received 21 October 2020; Revised 9 November 2020; Accepted 21 November 2020; Published 7 December 2020

Academic Editor: Barbara Gawdzik

Chitin was chemically extracted from crab shells and then dissolved in *N*,*N*-dimethylacetamide (DMAc) solvent with lithium chloride (LiCl) at 3, 5, 7, and 10%. The concentrated chitin-DMAc/LiCl solutions were used for the preparation of chitin hydrogels by water vapor-induced phase inversion at 20°C. The coagulation process was investigated while altering the concentration of LiCl in the DMAc solution. The shear viscosity of the chitin solution increased with higher LiCl amounts and decreased when the concentration of LiCl was reduced by adding water to the chitin solution, implying high LiCl concentration delayed the coagulation of chitin solution in the presence of water. The viscoelasticity of the chitin solutions indicated the gel formation intensification was dependent on the dose of LiCl and chitin in the DMAc solution. After the chitin solution was coagulated, the resultant hydrogels had water contents of 387–461% and the tensile strength varied from 285 to 400 kPa when the concentration of LiCl in the hydrogel was adjusted to 3% and 7%, respectively. As for viscoelasticity, the complex modulus of the chitin hydrogels indicated that the increment of the LiCl concentration up to 7% formed the tight hydrogels. Atomic force microscopic (AFM) image revealed the formation of the entanglement network and larger domains of the aggregated chitin segments. However, the hydrogel prepared at 10% LiCl in DMAc solution exhibited weak mechanical properties due to the loose hydrogel networking caused by the strong aggregation of the chitin segments.

1. Introduction

Hydrogels are defined as the hydrophilic structure being able to hold an excess amount of water inside their three-dimensional polymeric network [1–4], which can be classified based on different criteria, such as source, polymeric composition, configuration, and type of cross-linking [5]. The most common way to classify hydrogel is based on the material source. In the biomass hydrogel materials, natural polymers are available such as hyaluronic acid [6], alginate [7], chitosan [8], cellulose [1], chitin [2], and starch [9]. There are several advantages of biopolymer hydrogels. Especially, biopolymer hydrogel has the excellent biocompatibility and is better than other synthetic polymer-based hydrogel in medical applications. Biohydrogels have been demonstrated as a potential material in various fields due to its excellent strength, good compatibility, and degradation [10–15]. There are reports about the fabrication of the hydrogels with freeze-thawing process [3, 16], which are repeatedly performed at low temperature. However, the phase inversion method was successfully used to obtain biomass hydrogel contracting without cross-linker chemicals at room temperature [11, 14]. In this process, the biomass polymer is transformed in a controlled way from a solution state to a solid state by the solvent exchange in polymer solution to

nonsolvent, leading the polymer coagulation. Hence, the demixing process induces the formation and properties of the hydrogels. For example, the cellulosic hydrogels prepared by the phase inversion method in alcohol vapor showed the excellent mechanical properties and good biocompatibility [11, 17, 18]. Among the biomass-based hydrogels, chitin is the second most abundant polysaccharide composed of β-(1 ➡ 4)-*N*-acetyl-D-glucosamine unit (Figure 1). Favorite properties of chitin are being nontoxic, biocompatible, and biodegradable [13, 19]. In general, it has been known that the structure of chitin was stabilized by the strong intra- and intermolecular hydrogen bonds between chains, which made dissolving chitin difficult in common solvents [16]. While chitin cannot be dissolved in *N*,*N*-dimethylacetamide (DMAc) solvents, the addition of lithium salts can enhance the solubility of chitin [15, 20]. Chitin hydrogel has been known as a functional material which was applied in various fields such as biomedical [13], drug delivery [15], agricultural supporter as seed germination scaffold [16], and water treatment [2, 4]. However, the effects of LiCl concentration in DMAc solution for the chitin hydrogelation have not been clear. Most of the recent researches in preparation of chitin-based materials in DMAc solution were with the addition of LiCl at 5% (w/w) [21–26]. As seen from these studies, the reason for choosing the concentration of the added LiCl in DMAc solution has not been clear. Therefore, in the present study, the LiCl concentration in DMAc solution is investigated in the range of 3, 5, 7, and 10% to study the effect of LiCl on the formation of the hydrogels and on the properties of the obtained chitin hydrogels by using the phase inversion method under water vapor. Therefore, the resultant chitin solutions and hydrogels prepared from different LiCl concentrations were systematically investigated. Meaningful and original conclusions of the chitin hydrogel resulted in the phase inversion process. The properties of the chitin solutions were characterized in terms of viscosity with the addition of the coagulation water and viscoelasticity to observe the difference in the network formation between chitin segment and DMAc/LiCl solvent. For chitin hydrogels, the effect of LiCl concentration on the characteristics was measured in water content, mechanical strength, and topography with the surface roughness values to carry out the influence of the LiCl contents on the formation of the obtained hydrogels as the first report.

2. Materials and Methods

2.1. Materials. Crab shells were collected from snow crabs (genus Chinoecetes) in Teradomari, Niigata, Japan. All chemicals used in the preparation of chitin hydrogel were of analytical grade. Other chemicals, hydrochloric acid (HCl), sodium hydroxide (NaOH), potassium hydroxide (KOH), *N*,*N*-dimethylacetamide (DMAc), lithium chloride (LiCl), and ethanol which were products of Nacalai Tesque, Inc. (Tokyo, Japan), were used without any further purification. Prior to the use of DMAc, the solvent was stored with KOH for over 5 days and LiCl was dried in vacuum oven at 80°C in 24 h to remove trace of moisture.

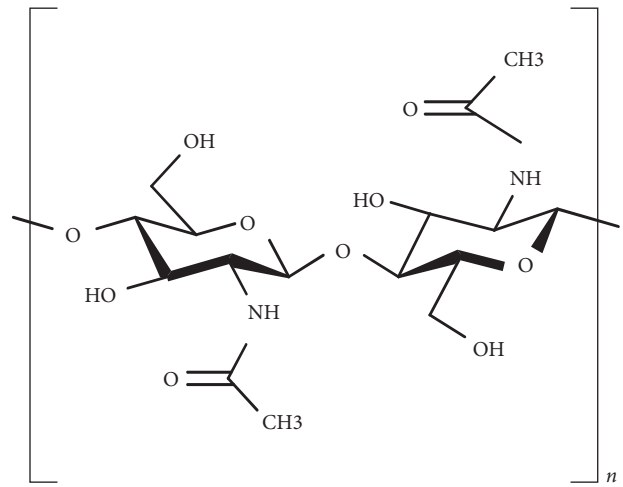

Figure 1: Chemical structure of chitin.

2.2. Preparation of Chitin Extracted from the Crab Shell Wastes and Chitin Hydrogels at Different LiCl Concentrations. Chitin used in the present work was chemically extracted from crab shell waste due to the increasing interest in the utilization of renewable feedstocks for chemicals with some modifications [27]. Figure 2 depicted the preparation process of chitin and the chitin-DMAc solution at different LiCl concentrations. In brief, in the demineralization process, 10 g of crab shells was treated with 300 mL of 1 N HCl aqueous solution at room temperature for 24 h. Then, deproteinization was carried out in 300 mL of 10% NaOH aqueous solution at 90°C for 5 h. Next, 300 mL of ethanol solution was added, and the crab shells were bleached at 60°C for 5 h. The solid part was filtered off and washed with distilled water to neutral pH. In comparison of the crab shells and the extracted chitin in Figure 2, it was clear that the decolorization was occurred in these purification processes. The fabrication of chitin hydrogel was carried out by the following process. Chitin was dissolved in DMAc/LiCl solvent for 5 days at room temperature. The LiCl content was adjusted in 3, 5, 7, and 10% in DMAc solution. Then, the concentration of the extracted chitin was added as 1 and 2% to the LiCl/DMAc solvent. Following that, the chitin solution was centrifuged at 9000 rpm in 30 minutes to remove the undissolved parts. After that, the chitin solutions were obtained in 1 and 2% of concentration. Figure 2 contained pictures of the chitin-DMAc solutions prepared at different concentrations of LiCl. For the hydrogel fabrication, the resultant chitin solution was casted on the Petri dish with 9.1 cm of diameter, which was placed in the plastic container ($12 \times 12 \times 6$ cm^3). Then, 40 mL of distilled water was also placed without contacting the chitin-DMAc solutions in the container. At room temperature, water vapor was induced in the wet-phase inversion process for the fabrication of the chitin hydrogels. After 24 h, the chitin hydrogel was formed in the Petri dish with DMAc solution. Before measurements,

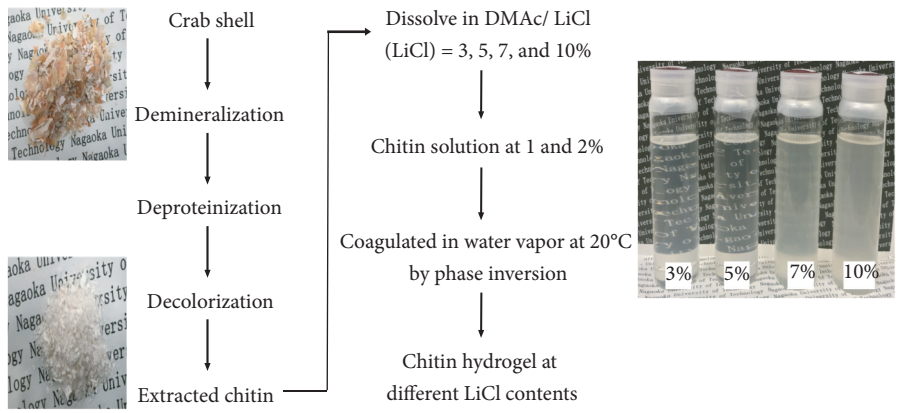

Figure 2: The preparation process of chitin, chitin-DMAc solution containing LiCl from 3 to 10% for C1-3 to C1-10, and chitin hydrogels with different LiCl concentrations.

all the obtained chitin hydrogels were washed with excess amount of distilled water several times to remove trace of solvent. For example, the chitin hydrogel sample prepared from 1% of chitin in 5% LiCl in DMAc solution was named as C1-5 signing with C (chitin concentration)-(% LiCl content).

2.3. Evaluation of the Chitin Solutions and Chitin Hydrogels Containing Various LiCl Concentrations. For the characteristics of the extracted chitin, chitin solution, and chitin hydrogels, several experiments have been carried out. Viscosity of the obtained chitin solutions was measured at 20°C as a function of the shear rate from 0.01 to 1000 s^{-1} by Rheometer (Physica MCR 301, Anton Paar). During the measurement, the exact amounts of water were added to the chitin-DMAc solution to demonstrate the change in the viscosity values. Rheology of the chitin solutions having different LiCl concentrations was measured as a function of the frequency from 0.01 to 100 Hz, while the strain was 1% at 20°C. Fourier-transform infrared spectroscopy (FT-IR) spectra were recorded with JASCO FT-IR/4100 spectrometer by grinding dried samples with potassium bromide (KBr) in the absorbance model and taken from 4000 to 500 cm^{-1} wavelengths with the resolution of 2 cm^{-1}. The degree of acetylation (DA) of the resultant chitin was calculated according to the method [28] by the following equation:

$$\text{DA } (\%) = \frac{(A_{1650}/A_{3450})}{1.33} \times 100. \quad (1)$$

Here, A_{1650} and A_{3450} were referred to the absorbance of peak at 1650 and 3450 cm^{-1}, which related to the bands of amide I and hydroxyl group, respectively, in the FT-IR spectra. The deconvolution of the FT-IR spectra in the range of 3700–3000 cm^{-1} was carried out. The center of the fixed peaks obtained from the spectral data was decomposed into their Gaussian components. The peal centers and the curve were then fitted using OriginPro 8.5.

The values of water content (WC) of the hydrogels were measured at room temperature by immersing 30 mm × 10 mm strips of the dry hydrogels in distilled water. After the soaking period was 24 h to ensure equilibrium sorption, the hydrogels were removed and quickly wiped with tissue paper and finally weighed. The value of WC was calculated for each sample using the following equation:

$$\text{WC } (\%) = \frac{(m - m_0) \times 100}{m_0}, \quad (2)$$

where m_0 was the dry weight and m was the weight of the hydrogels after 24 h immersion in distilled water.

Atomic force microscopy (AFM) measurement was performed with samples (10 mm × 10 mm) in the wet conditions by using the cantilever (SI-DF3-A). The scanning area was 5 μm^2 for measuring the topography of the hydrogel surface with the root mean square values (RMSs).

The mechanical properties of the resulting hydrogels were evaluated with tensile strength and viscoelasticity. In the tensile strength, the test was carried out by using LTS-500N-S20 (Minebea, Japan) with an operating head load of 500 N at 23°C and 50% RH. The wet hydrogel specimens (40 mm × 10 mm) were then placed between the grips of the testing machine. The initial length was 20 mm, and the speed of testing was 2 mm min^{-1} till the sample was broken. The values of tensile strength and elongation were calculated using the following equations:

$$\text{tensile strength} \left(\frac{N}{mm^2}\right) = \frac{\text{maximum load}}{\text{cross} - \text{sectional area}}, \quad (3)$$

$$\text{elongation } (\%) = \left(\frac{\text{elongation at rupture}}{\text{inintial gauge length}}\right) \times 100. \quad (4)$$

Viscoelasticity of the wet hydrogels was conducted at 20°C to obtain the complex modulus (G^*) of the samples as a function of frequency (Hz) of 0.01–100 Hz and strain (%) from 0.01 to 100%.

3. Results and Discussion

3.1. Properties of the Extracted Chitin and Chitin in the DMAc Solution with Different LiCl Concentrations. The crab shells were light reddish after the chemical treatment, as shown in Figure 2. The yield of the purification from crab shells was

gained about 34.7 ± 2.1%, and the value of DA for the extracted chitin was calculated as 73.4 ± 5.2%. As shown in Figure 2, the chitin-DMAc solution had yellowish color and the transparency was somewhat decreased when the LiCl concentration was up to 7–10%. The shear viscosity of the obtained chitin solution was measured at various concentrations of LiCl/DMAc solution as a function of the shear rate (Figure 3). It was observed that the amounts of LiCl concentration in the DMAc to chitin solution had a strong effect on the viscosity. As seen, at the shear rate of 0.1 s^{-1}, the values of viscosity were increased as 0.17 and 4.9 Pa.s for C1-3 and C1-10 solutions, respectively. When the chitin concentration was 2%, the viscosity was 0.2 Pa.s for C2-3 and 7.5 Pa.s for C2-10 solutions. It was remarkable that when the LiCl concentration in the DMAc solution was 3%, the viscosity was significantly low for C1-3 and C2-3, respectively. This could be due to the lack of LiCl content in DMAc, which led to the deficient interaction to chitin segments. Therefore, the chitin solutions prepared at 3% LiCl concentration were extremely diluted. However, when the LiCl concentration was 10%, the values of viscosity were significantly enhanced. This could be attributed to the macrocation formed in the DMAc/LiCl system, which interacted with chitin molecules and acted as cross-linker as well as in the case of cellulose [14]. In this study, the result was seen that higher concentration of chitin in the DMAc solution also caused the increment of the shear viscosity of the related solutions. For example, at 0.63 s^{-1} of the shear rate, the viscosity of C2-5 was 2.8 Pa.s, while the value of C1-5 was 0.74 Pa.s. Increasing the shear rate up to 10 s^{-1} caused the decrease in viscosity as 0.68 and 1.12 Pa.s for C1-5 and C2-5, respectively. This indicated that a higher shear rate deformed the hydrogen bonding between chitin segments. As a result, the presence of LiCl in the DMAc solution could be dissoluble causing chitin to extend its molecular shape in DMAc.

To study the effect of the added water on the chitin-dissolved DMAc/LiCl solution, viscosity was measured, when the amount of the added water was changed. During the measurement of the viscosity, the shear rate was kept at 0.63 s^{-1}. Figure 4 illustrates the viscosity at different ratios of the added water and the chitin-DMAc solutions in the range from 0 to 10. As a result, the added water in the chitin solution caused the increment in the shear viscosity through the turning point of the viscosity decreased, corresponding to be on the starting process of gelation. When the added amounts of the water further increased, the tendency on the viscosity decreased, meaning that the chitin in the DMAc solution was coagulated. This might be due to the effective solvation of the water to the formation of the macrocation of chitin and LiCl in DMAc solution. In particular, the shear viscosity was increased from 0.17 to 5.5 Pa.s for C1-3 and 0.74 to 6.4 Pa.s for C1-5 at water: DMAc/LiCl of 0 and 2, respectively. Afterwards, the values were decreased when the ratio of the added water and chitin-DMAc solution (water: DMAc/LiCl) reached 4 and 5. It could be because the higher amount of the added water caused the faster gelation of the chitin in the solution. Meanwhile, the opposite tendency was seen in the cases of C1-7 and C1-10. When the ratio between

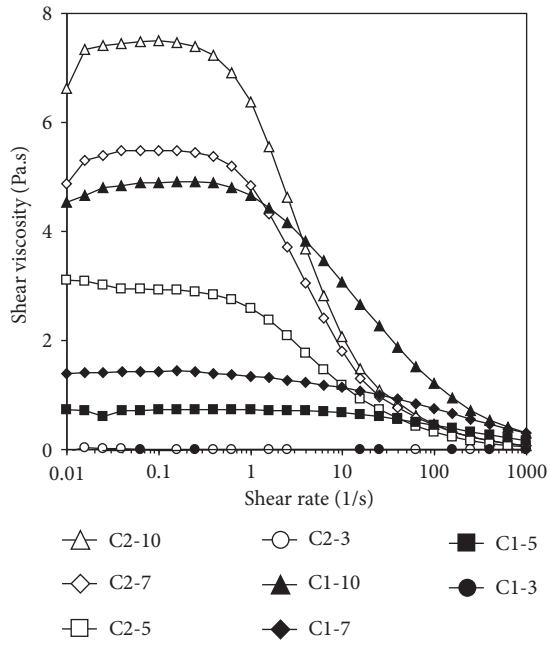

Figure 3: Shear viscosity of the chitin solutions prepared at different LiCl concentrations.

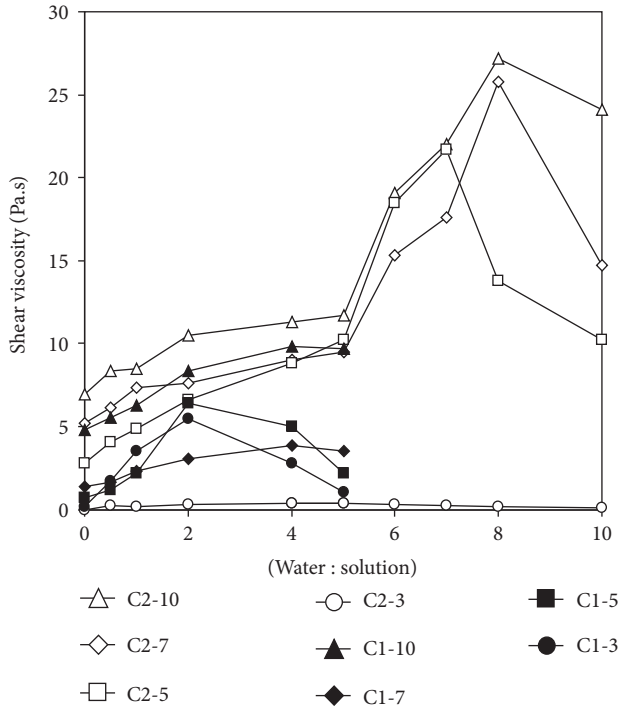

Figure 4: Shear viscosity of the chitin-DMAc solution with the added water in different amounts at 0.63 s^{-1} of the shear rate.

the added water and chitin-DMAc was changed from 0 to 4, the increment in the shear viscosity was seen. For instance, the obtained values were 1.4 and 3.9 Pa.s for C1-7 and 4.8 and 9.8 Pa.s for C1-10 at water: DMAc/LiCl as 0 and 4, respectively. However, when the ratio reached water: DMAc/LiCl as 5, the values of viscosity were observed as 3.5

and 9.7 Pa.s for C1-7 and C1-10. It was noted that higher concentration of LiCl might contribute to the higher water retention causing the longer constant viscosity. For C1-3 and C1-5, the gelation point was seen at the water: DMAc/LiCl as 2, while higher LiCl concentration caused the higher point at water: DMAc/LiCl as 4 for C1-7 and C1-10. The similar tendency for 2% of chitin solution had higher values relative to 1% of chitin solution. When the added water was increased to 2% chitin concentration, the C2 solution was observed with the increment of shear viscosity up to the ratio of 5. Nevertheless, more addition of water reduced the values of the viscosity. The gelation points were obtained at water: DMAc/LiCl as 5 for C2-3 was 0.39 Pa.s, while the viscosity value was 0.29 Pa.s obtaining at water: DMAc/LiCl as 6. The values of the shear viscosity of the C2-3 solution with the addition of water seemed to be constant. It could be because of the deficient interaction of LiCl content in DMAc solution to chitin segment. Low LiCl concentration in DMAc solution could not enable the effective dissolution of chitin molecules in the preparation process, indicating the low viscosity observed in Figure 3. For C2-5 solution, the viscosity was decreased from 21.7 Pa.s to 13.8 Pa.s when the ratio of water: DMAc/LiCl was 7 and 8, respectively. At a higher LiCl concentration at 7 and 10%, the higher gelation points were seen at the water: DMAc/LiCl as 8 for 25.8 Pa.s in C2-7 and 27.2 Pa.s for C2-10, meaning the strong retention of chloride ion in the macrocation to water molecule. When the ratio of water: DMAc/LiCl was 9, the related viscosity reduced as 14.7 Pa.s and 24.1 Pa.s for C2-7 and C2-10, respectively. After adding water to the chitin-DMAc solution, the decreased viscosity meant the insoluble chitin gelation in the DMAc solution. It might be due to the enhancement in the chitin concentration leading to the higher intensity of the gelation process due to the strong affinity of water molecules to chitin segment to induce gelation. It was noted that the gelation of chitin solution was delayed in the presence of the added water when the LiCl concentration was high in DMAc solution. This suggested that the highly solvated macrocation to chitin delayed the demixing process in the addition of water.

Figure 5 depicts the viscoelasticity of the chitin-DMAc solution as a function of frequency from 0.01 to 100 Hz. The rheological properties of the chitin-DMAc solution having the LiCl concentration at 3, 5, 7, and 10% were carried out at 20°C, and the strain was 1%. Figure 5(a) represents the storage modulus (G') and loss modulus (G'') of the C1 chitin solutions as a function of the frequency from 0.01 to 100 Hz. The values of G' and G'' increased gradually with the increment of frequency especially in the C1 samples. Here, the chitin solution prepared at 3% LiCl showed the viscous behavior, as G'' was higher than G'. As seen, the G' depended on the frequency remarkably. Interestingly, with the increase in the LiCl concentration from 5 to 10%, the values of the G' decreased as 8.4, 4.2, and 4.3 Pa for C1-5, C1-7, and C1-10 at 1 Hz, respectively. The gelation process was able to occur when G' became higher than G''. When the G' was higher than the G'', the point was for the gelation point. Here, the crossover point between G' and G'' was moved to a higher frequency with the enhancement of the LiCl concentrations. With the addition of LiCl from 5 to 10% in the chitin-DMAc solution, the crossover frequency was seen at 2.2 and 6.8 Hz, meaning that the relaxation time was decreased due to the increment in entanglements in the chitin/LiCl/DMAc solution [29]. It has been reported that high LiCl amount in DMAc solution could form the macrocation $[\text{DMAc-LiCl-DMAc-Li}]^+$–$\text{Cl}^-$, which acted as a cross-linker with chitin segments [14]. Therefore, longer time is required to obtain the gel formation as seen in the viscosity results. At a higher concentration of chitin solution, the G' value was increased as 21.8 Pa for C2-5 at 1 Hz in Figure 5(b). However, the G' was not different as 21 Pa for C2-7 and C2-10. It was noted that the chitin solutions prepared with 5% LiCl showed the highest values of G' in the C1 and C2 solutions, suggesting the stronger gel intensity. In addition, G' was considered to be the indicator of the gel-network extend. Therefore, the higher G' meant the stronger gel intensity. Moreover, the tan $\delta = G''/G'$ was calculated. Figure 5(c) describes the value of tan δ of chitin solutions as a function of frequency. The decrease in tan δ for all the samples indicates the shift of the materials towards the increment of elastic as the frequency and the chitin concentration increased. For the C1 solution, the tan δ was seen to be decreased as 2.41, 0.92, 1.26, and 1.3 when the LiCl content increased from 3 to 10%, respectively. When the chitin concentration was changed to 2%, the values of tan δ were reduced to 3.16, 0.6, 0.65, and 0.63 for the C2-3, C2-5, C2-7, and C2-10, respectively.

3.2. Properties of Chitin Hydrogels Prepared from Different LiCl Concentrations. Figure 6 shows the appearance of the chitin hydrogels prepared from 1% chitin concentration. Here, for the C1 samples, the round-shaped hydrogels were prepared in the round Petri dish with 9.1 cm diameter in the water vapor conducted at 20°C. Here, the images of the samples were taken after the gelation finished without washing in distilled water. The diameter of the hydrogel was increased, when the addition of LiCl content was higher. For example, the diameter and thickness for the sample having 3% of LiCl content were 44 and 0.7 mm, respectively. Meanwhile, the values were increased as 65.6 mm for diameter and 1.1 mm for thickness in the case of C1-10. This suggested that the formation of the macrocation $[\text{DMAc-LiCl-DMAc-Li}]^+ - \text{Cl}^-$ influenced the chitin hydrogel formation, especially at higher concentration of 10% LiCl in DMAc solvent [14]. So the Cl^- ion could be hydrated, exhibiting strong swelling interactions with water molecules [30]. Therefore, the hydrogel could absorb water during the solvent-exchange process in the closed space. Figure 7 shows the formation of the macrocation $[\text{DMAc-LiCl-DMAc-Li}]^+$ and the hydration between Cl^- and water molecules. As seen, at 10% of LiCl concentration, the obtained chitin hydrogel gained the higher diameter of the appearance due to the water retention of Li^+ and Cl^- ions. The diameter and thickness of the chitin hydrogels prepared at different LiCl contents are listed in Table 1.

By the results of demixing of the DMAc-water in the chitin solution, the hydrogels are obtained, as shown in

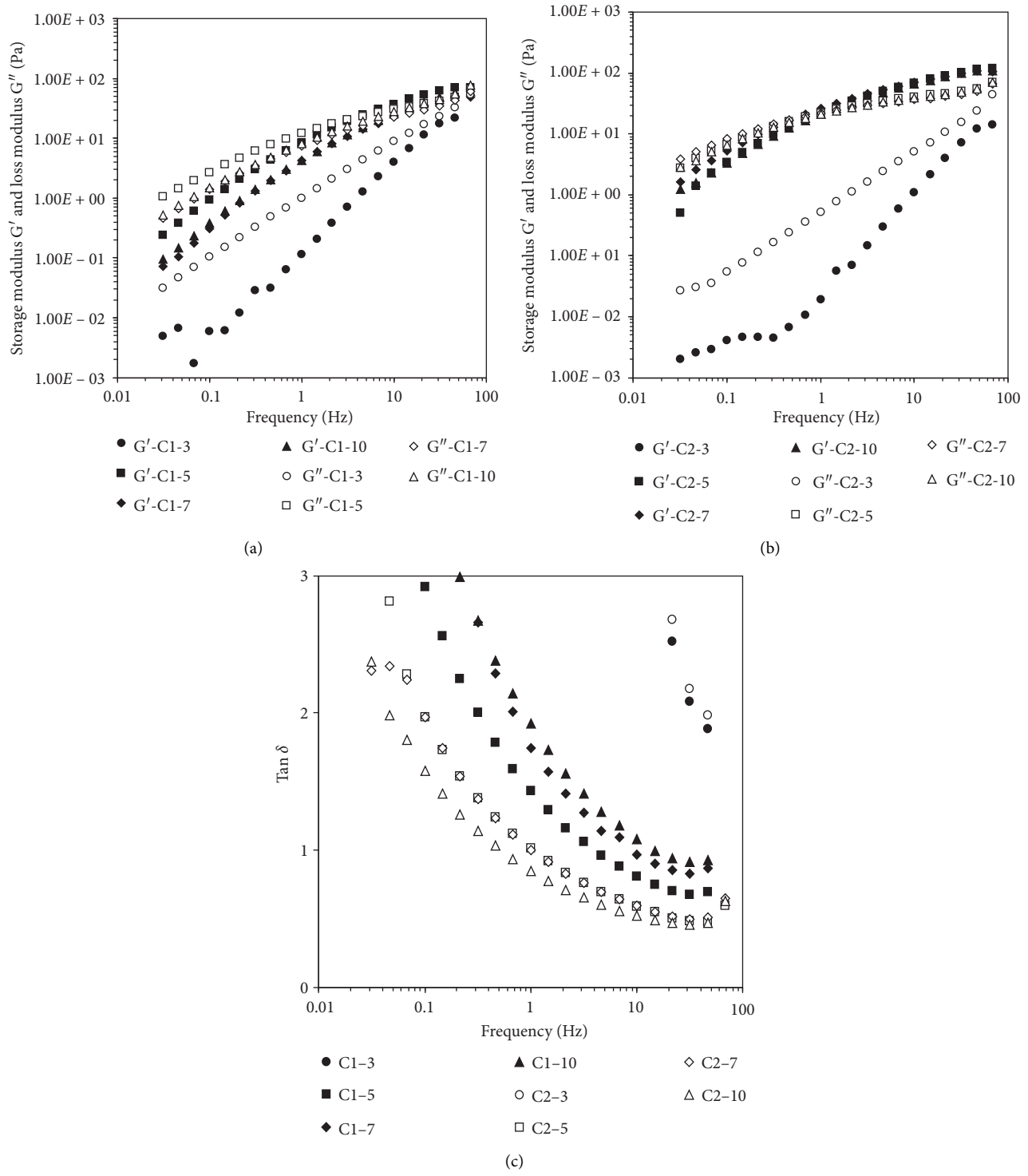

Figure 5: The viscoelasticity of chitin-DMAc solutions containing different LiCl concentrations for (a) C1 and (b) C2 and (c) tan δ as a function of frequency.

Figure 6. Before measurements, the chitin samples were washed in excess amount of diluted water to remove traces of solvent. Here, the water content of the chitin hydrogel decreased with the increment in LiCl concentration, and the value was reduced from 461 to 388% for C1-3 and C1-10, respectively, as shown in Table 1. However, the lower value obtained for C1-5 and C1-7 was 370% and 343%, respectively. It might be because of the water-washing process of hydrogel leading to the macrocation elimination from the hydrogel. The complex between the $[DMAc–Li]^+$ ion and the chitin molecule was decomposed through solvation by water. As a consequence of reduced solvent power, chitin

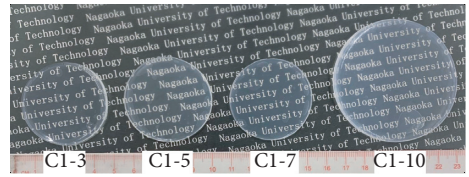

Figure 6: The appearance of the chitin hydrogels at different LiCl concentrations.

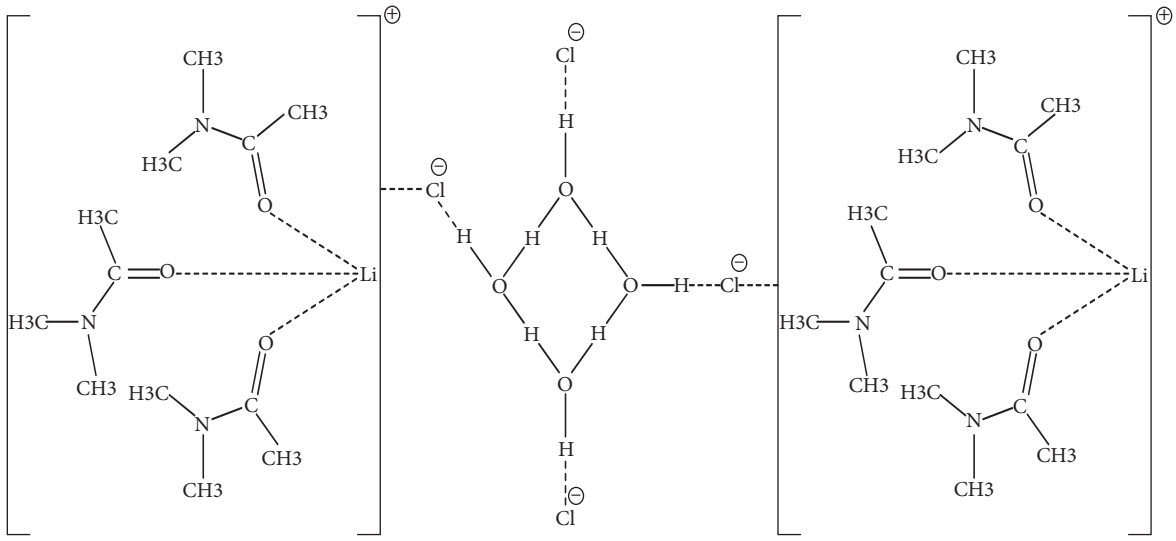

Figure 7: The formation of the macrocation $[DMAc\text{-}LiCl\text{-}DMAc\text{-}Li]^+$ and the hydration between Cl^- ion and water molecules.

Table 1: Characteristics of the chitin hydrogel prepared at various LiCl contents.

Sample	Diameter (mm)	Thickness (mm)	Water content (%)	CI (%)	Tensile strength (kPa)	Elongation (%)
C1-3	44 ± 1.5	0.7 ± 0.01	461 ± 25	72 ± 4	285 ± 7	65 ± 2
C1-5	44.5 ± 1.7	0.75 ± 0.01	370 ± 13	48 ± 3	380 ± 8	79 ± 5
C1-7	44 ± 0.5	0.85 ± 0.03	343 ± 30	66 ± 4	400 ± 9	78 ± 2
C1-10	65.5 ± 0.5	1.11 ± 0.02	388 ± 12	73 ± 5	134 ± 7	34 ± 1
C2-3	46 ± 1	0.76 ± 0.02	484 ± 3	73 ± 2	358 ± 7	55 ± 3
C2-5	46 ± 1.6	0.8 ± 0.02	427 ± 13	58 ± 3	729 ± 6	65 ± 4
C2-7	46.5 ± 1	0.84 ± 0.03	359 ± 6	67 ± 2	685 ± 6	69 ± 4
C2-10	66.5 ± 1.1	1.24 ± 0.02	332 ± 13	73 ± 3	276 ± 5	34 ± 1

molecules were phase-separated from solution, forming an associative network through attractive segment-segment interactions. Physical crosslinks formed as a result of hydrogen bonding interactions, namely, forming intra- and intermolecular hydrogen bonding [25]. Hence, the water content of C1-7 and C1-10 was not significantly different. Similar results were seen when the concentration of chitin was 2% in the solution, and the water retention was reduced from 484 to 332% when the LiCl concentration was changed as 3 and 10% LiCl for C2-3 and C2-10, respectively. In the case of cellulose hydrogel fabricated in LiCl/DMAc solution, the similar tendency was observed with the reduction of water content as the LiCl content increased [14]. The values of the water content of the hydrogel prepared at different LiCl concentration are listed in Table 1.

Figure 8 depicts the FT-IR spectra of the (a) extracted chitin, (b–e) C1, and (f–i) C2 hydrogel samples from 500 to 4000 cm^{-1} of wavelengths. As seen in Figure 8, (a) displayed the specific functional groups in the purified chitin for the O–H stretching band at 3425 cm^{-1}, amid I band at 1654 cm^{-1}, amide II (N–H) stretching at 3265 and 1552 cm^{-1}, the C–H bonding at 2888, 2932, and 2960 cm^{-1}, and the C–O stretching and the C–O–C ring related at the peak of 1025 and 1155 cm^{-1}, respectively. Two amide I bands observed at 1654 and 1623 cm^{-1} suggested the α-form of the extracted chitin [31]. As seen in the IR spectra of the hydrogel sample prepared with 1% and 2% chitin concentrations as for C1 (Figure 8, (b–e)) and C2 (Figure 8, (f–i)), each functional group was well remained after the dissolution in LiCl/DMAc solution.

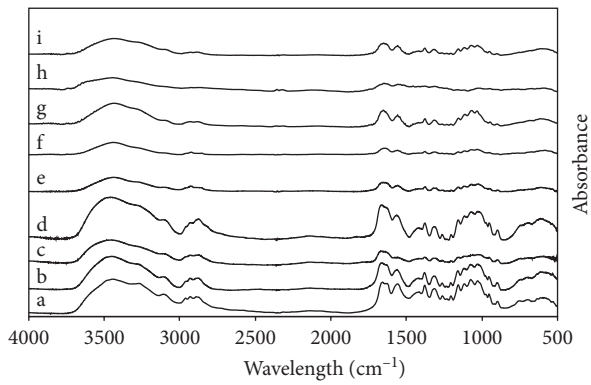

Figure 8: FT-IR spectra of the (a) extracted chitin, (b–e) C1-3 to C1-10, and (f–i) C2-3 to C2-10.

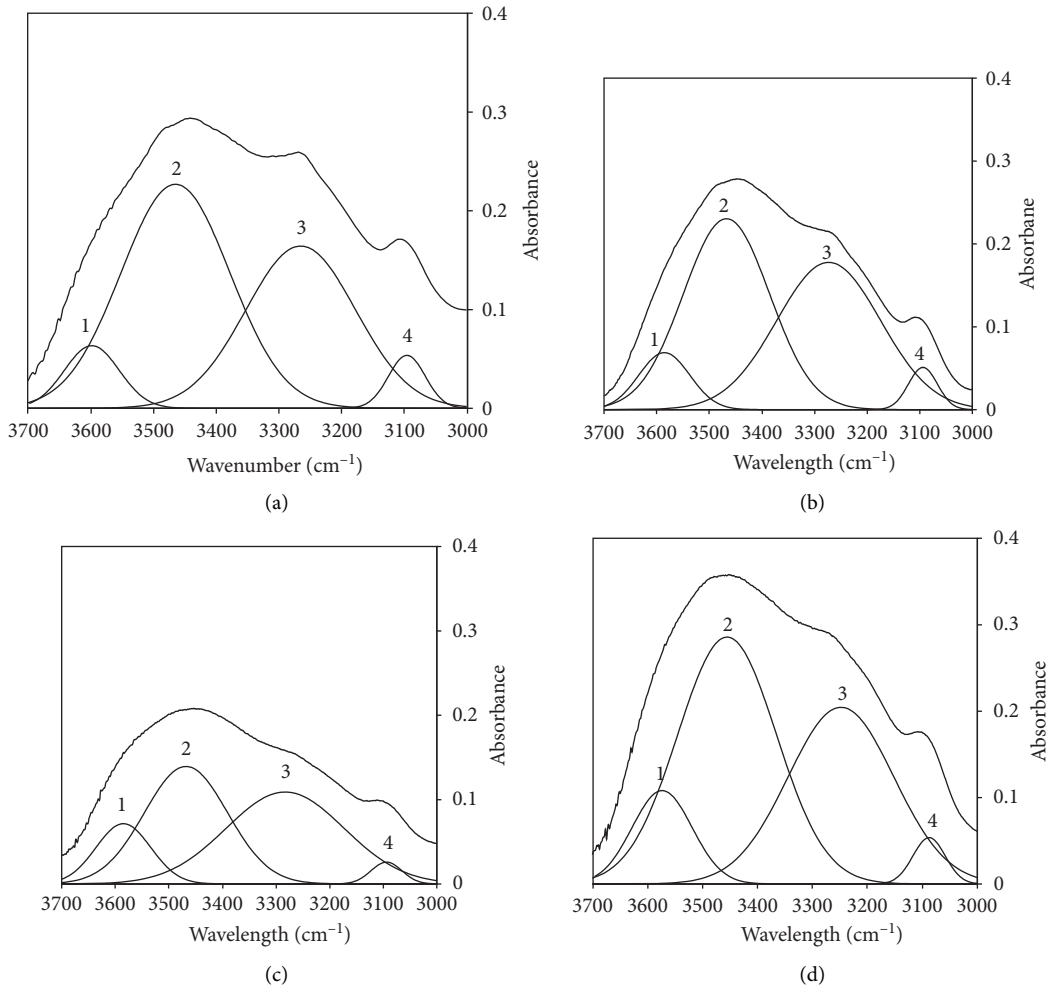

Figure 9: Continued.

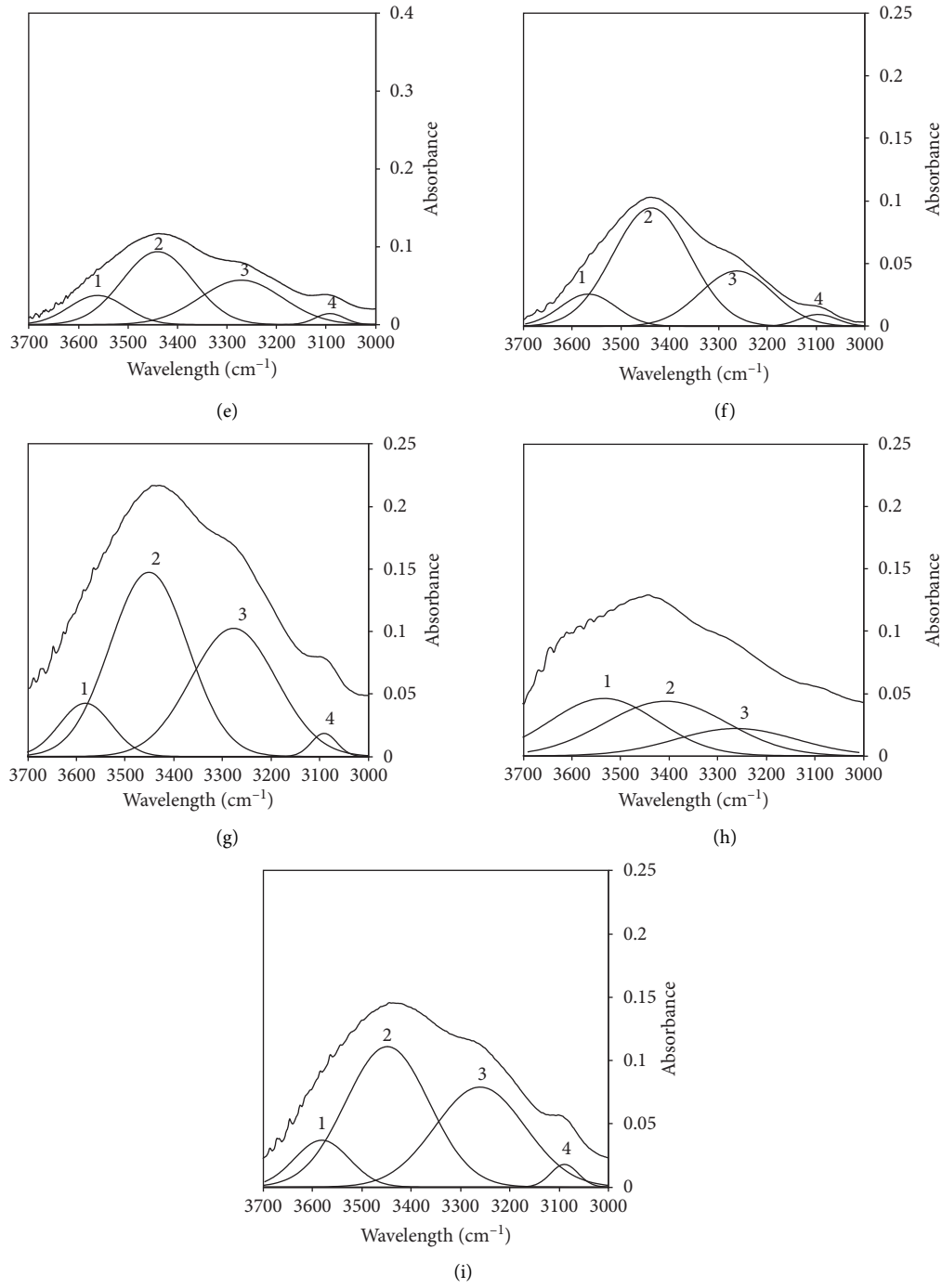

Figure 9: Deconvolution FT-IR spectra of (a) the extracted chitin and chitin hydrogel of (b–e) C1-3 to C1-10 and (f–i) C2-3 to C2-10.

It was interestingly noted that the FT-IR spectra for chitin hydrogel obtained at various LiCl concentrations had somewhat differences in the range of 3000–3700 cm^{-1}. Therefore, the deconvolution was carried out using the second derivative method. These spectra were decomposed into Gaussian components by curve fixed positions. Figure 9 shows the fixed curves of (a) extracted chitin and chitin hydrogels of (b–e) C1 and (f–i) C2. Normally, chitin extracted from crab shells, as seen in Figure 9(a), had two intramolecular hydrogen bonds C(6)–OH$\cdots$O–C (peak 1) at 3597 cm^{-1} and C(3)–OH$\cdots$O–C(5) (peak 2) at 3464 cm^{-1}. In addition, the structure of the α-chitin was stabilized by two intermolecular hydrogen bond NH$\cdots$OC (peak 3) at 3265 cm^{-1} and C(6)–OH$\cdots$OH–C(6) (peak 4) at 3095 cm^{-1} [32–34]. It was noted that the large portion of C(3)–OH$\cdots$O–C(5) and NH$\cdots$OC was dominant in the bands in the hydrogen bonding networks. For the extracted chitin (Figure 9(a)), the portion values of peak 2 and peak 3 were 51.3 and 37.5%, respectively, while those of the hydrogel samples were decreased as 46% for C1-3 and 48% for C1-7

and C1-10 and became the lowest one of 39.9% for C1-5 in the case of peak 2 (Figures 9(b)–9(e)). This indicated that the DMAc/LiCl solvent could reduce the hydrogen bonding of the intramolecular bonding (peak 2). However, the higher LiCl concentration seemed not to effectively disrupt the hydrogen bonding network of the chitin segments due to the formation of the macrocation cation [DMAc-LiCl-DMAc-Li]$^+$. This complex was solvated by water molecules very well, resulting in a drastic decrease in solvent power. After that, the chitin segment tended to phase separate from the solution quickly. Water molecules intruded with the degree of intra- and intermolecular hydrogen bonding among chitin chains. Therefore, at higher LiCl concentrations of 7 and 10% in DMAc solution, the increment in the intramolecular hydrogen bonding was obtained because of the interaction of chitin segment. Also, the portion of the intermolecular hydrogen bonding at peak 3 was different in each hydrogel. For example, the portion of peak 3 was 42.5% for C1-3 and 44.1% for C1-5 and lower values as 37.3% for C1-7 and 34% for C1-10. It seemed that LiCl concentration more than 5% in DMAc solution could cause the better intramolecule bonding of chitin segment. Therefore, the C1-5 had the highest storage modulus in association with the highest gel intensity among all the C1 samples due to the larger portion of intermolecular hydrogen bonding. For the deconvolution of the C2-3 to C2-10 hydrogels, similar tendency was recorded for the portion of peak 3, as intermolecular hydrogen bonding of C2-5 was higher than those of the others. The area portion of the chitin hydrogels is listed in Table 2.

Since such interaction of chitin segment in the hydrogel influenced the morphology such as surface area, AFM measurements were carried out in the wet condition. Figure 10 shows the AFM images at 5 μm^2 scanning area with the wet condition of the chitin hydrogels for C1-3 to C1-10 (Figures 10(a)–10(d)) and C2-3 to C2-10 (Figures 10(e)–10(g)). For the C1 samples, the addition of LiCl in the DMAc solution caused the difference in size distribution of the chitin fiber on the surface of the hydrogels. The chitin hydrogel containing 3% LiCl showed the ordered distribution of the chitin segments on the surface of the hydrogel with the RMS was 85.1 nm for the C1-3 and became somewhat fine morphology with RMS as 15 nm for C1-5. With the increment in the LiCl concentration to 7 and 10%, the segment morphology seemed to be aggregated. It was observed that the larger domains of chitin segments were present on the hydrogel surface. In addition, the RMS values of C1-7 and C1-10 were 44.8 and 62.8 nm, respectively. In the results of the deconvolution FT-IR spectra, the highest portion of the intermolecular hydrogen bonding was observed when the chitin hydrogel was prepared at 5% LiCl content in DMAc solution. This suggested the intermolecular hydrogen bonding between the chitin segments could enable the stronger entangled network of the chitin fiber, causing the lowest RMS values. There was tendency that when the LiCl concentration increased, the chitin segments aggregated as well as cellulose, which was observed previously [14]. As mentioned in Figure 9, the portion of the intramolecular interaction of chitin molecules was somehow higher at 7 and 10% LiCl in DMAc solution, suggesting the larger domains of chitin segments were formed by the aggregation of chitin fiber on the hydrogel surface. The chitin concentration also affected the RMS values. The chitin segments network of C2 samples had better distribution than those of C1 as the RMS values were lower indicating the intensification of the chain entanglement. For example, the RMS for C2-3 was 59.3 nm while as 27.6 nm for C2-5, as seen in Figures 10(e)–10(f). At a higher LiCl concentration in the hydrogel, the RMS increased as 31.2 nm for C2-7 (Figure 10(g)) and 50.5 nm for C2-10 (Figure 10(h)). Therefore, the increment in chitin concentration caused the stronger gel formation of the hydrogel due to the higher solvation of LiCl/DMAc solution to chitin.

Figure 11 shows the XRD pattern of the extracted chitin and chitin hydrogel at 3, 5, 7, and 10% of LiCl when the chitin concentration was 1%. As seen, the XRD result of the prepared chitin showed the peak at $2\theta = 9.3^\circ$, 12.6°, 19.2°, 22.5°, and 26.2° for diffraction planes of chitin at (020), (021), (110), (130), and (013). This indicated the crystalline structure of α-chitin [16]. After the chemical treatment, the CI of the purified chitin was calculated as 88%. Here, the chitin hydrogel prepared at different LiCl contents also indicated the similar peak compared to the extracted chitin. As listed in Table 1, the CI of the chitin hydrogel was affected by the LiCl amount. The CI of the chitin decreased after dissolving in DMAc and LiCl [35]. For example, the CI was reduced to 72% for C1-3 and the lowest value as 48% in the case of C1-5. Here, the CI increased as 63 and 71% for C1-7 and C1-10, respectively. The XRD patterns for C2 hydrogel also exhibited the similar typical peaks. However, the CI was different as 58% for C2-5. At low LiCl concentration as 3%, it may due to the lack of interaction between LiCl and DMAc to solvate the chitin segment. On the other hand, the hydrogel prepared with 7 and 10% LiCl in DMAc solution showed the entangeled network of chitin segments on the hydrogel surface as seen in the AFM images. Therefore, the CI values increased due to the stronger aggregation of chitin segments formed by the intramolecular interactions between them. The values of CI are shown in Table 1.

As presented in Table 1, the tensile strength and elongation of the chitin hydrogel contain various LiCl contents from 3 to 10%. Apparently, the loading of LiCl increased from 3 to 7% causing the enhancement of the mechanical property of the hydrogels. For example, the values of the tensile strength and elongation were increased from 285 kPa and 64.6% to 400 kPa and 78% for C1-3 and C1-7, respectively. The tensile strength of C1-5 was 380 kPa with 79% of elongation. The entangled network of the hydrogel was intensified by the domains of chitin segments at a higher chitin concentration, consequently reflecting the mechanical properties. As seen, increasing the chitin concentration in DMAc solution caused the better mechanical property of the hydrogels. The tensile strength and elongation were increased as 358 kPa and 55% for C2-3, 729 kPa and 65% for C2-5, and 685 kPa and 69% for C2-7, respectively. For the hydrogels prepared at 10% LiCl, the values of the tensile strength and elongation were 134.2 kPa and 34% for C1 and 275 kPa and 34% for C2. The less

Table 2: Area portion (%) of the hydrogen bonding in the region of 3700–3000 cm^{-1} in the deconvolution FT-IR spectra.

Peak	% area								
	Extracted chitin	C1-3	C1-5	C1-7	C1-10	C2-3	C2-5	C2-7	C2-10
1	7.1	8.1	13.3	11.1	15	11.5	9.6	27	10.6
2	51.3	46	39.9	48.6	48	59.2	50	42.3	49
3	37.5	42.5	44.1	37.3	34	26.3	38.3	30.7	37.7
4	4.1	3.4	2.7	3	3	3	2.1	0	2.7

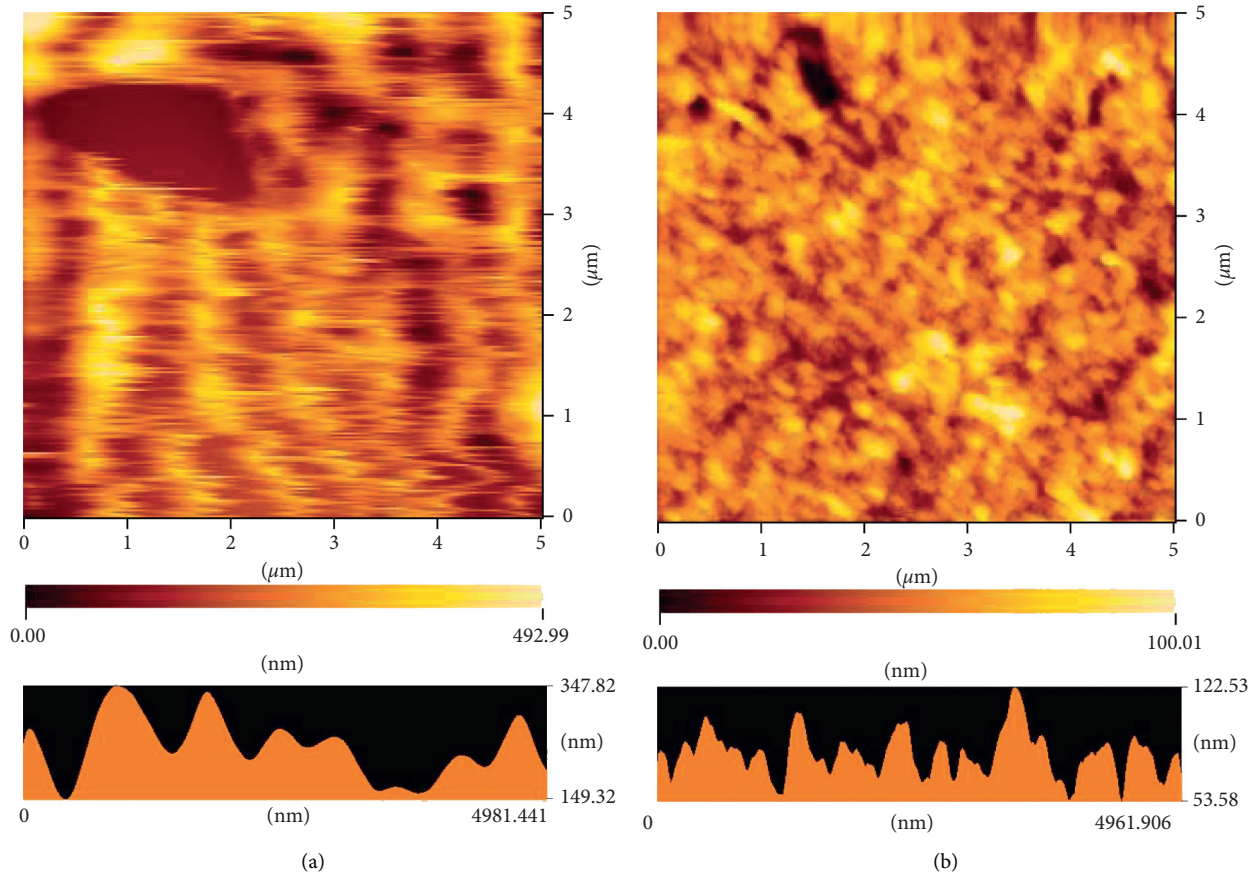

Figure 10: Continued.

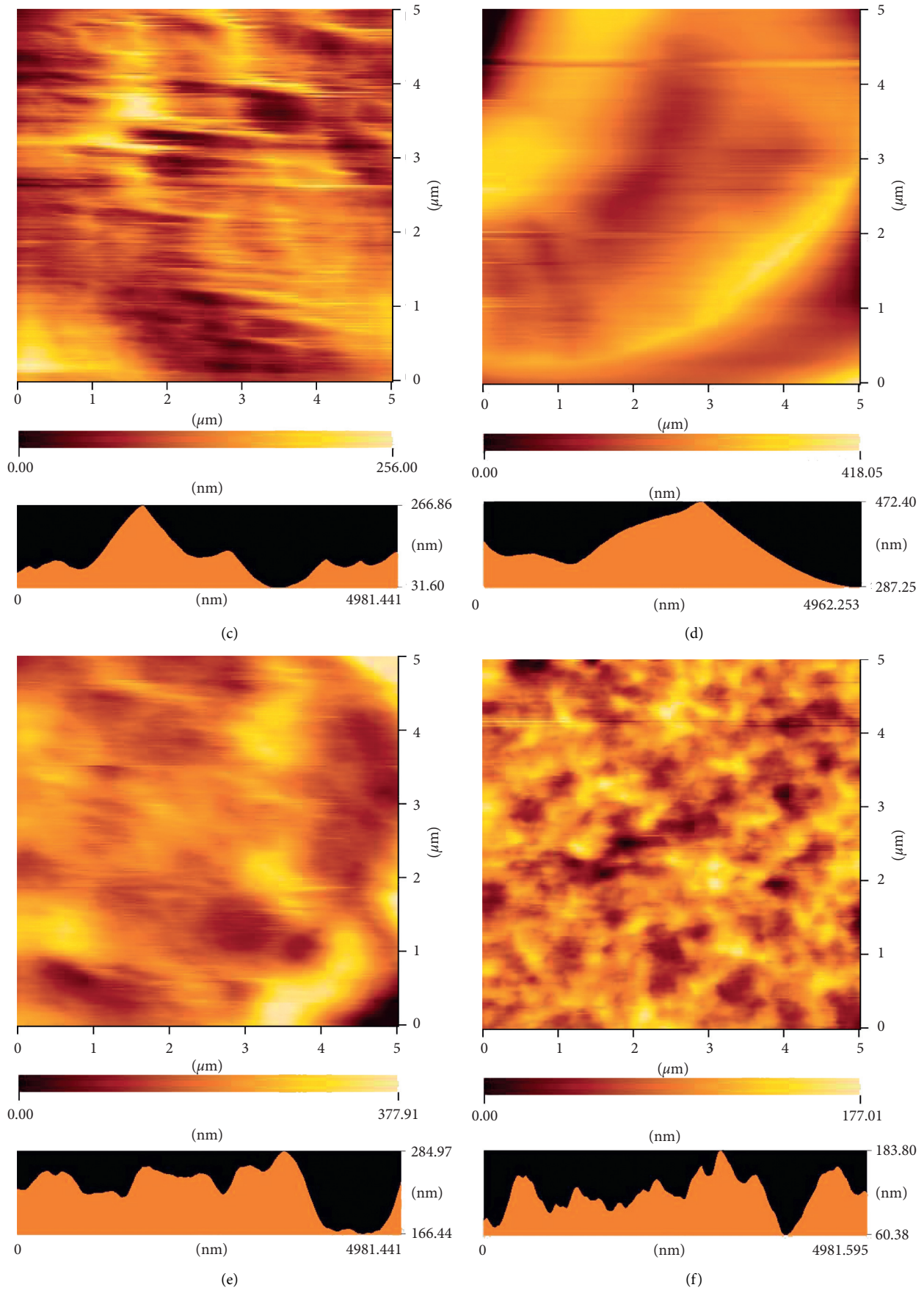

Figure 10: Continued.

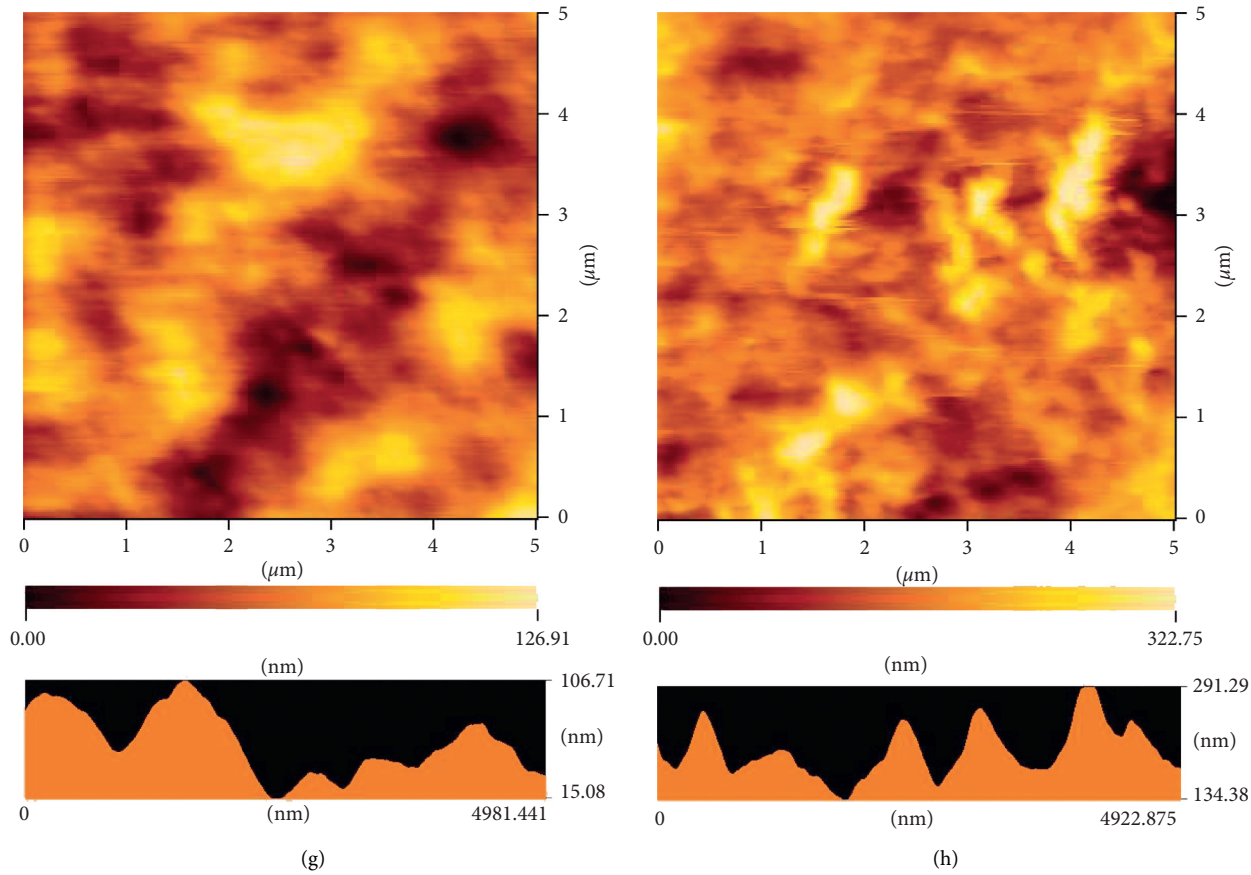

Figure 10: AFM images of the chitin hydrogel (a–d) C1-3–C1-10 and (e–h) C2-3—C2-10 at 5 μm^2 scanning area.

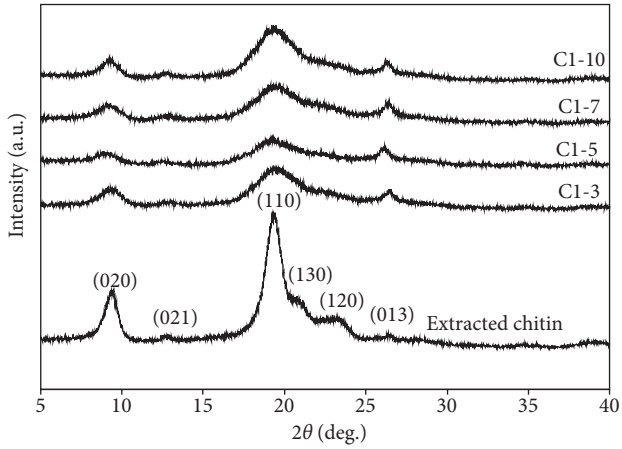

Figure 11: XRD patterns of the extracted chitin and the C1 hydrogel samples.

solvation of the chitin segments led to the aggregated formation of the chitin segments, as seen in the AFM images. In addition, the large domains of the aggregated chitin part could cause the loose of interconnection of chitin segment, resulting in the low inter- and high intramolecular hydrogen bonding, as seen in the FT-IR. Therefore, the hydrogel film prepared at 10% LiCl concentration exhibited the low mechanical properties due to the soft structure.

Figure 12 exhibits the complex modulus (G^*) of the chitin hydrogels as a function of the frequency from 0.01 to 100 Hz and strain from 0.01 to 100%. The tendency of G^* at 0.1 Hz frequency was observed that the values of all the hydrogels were higher up to 7% LiCl concentration for the

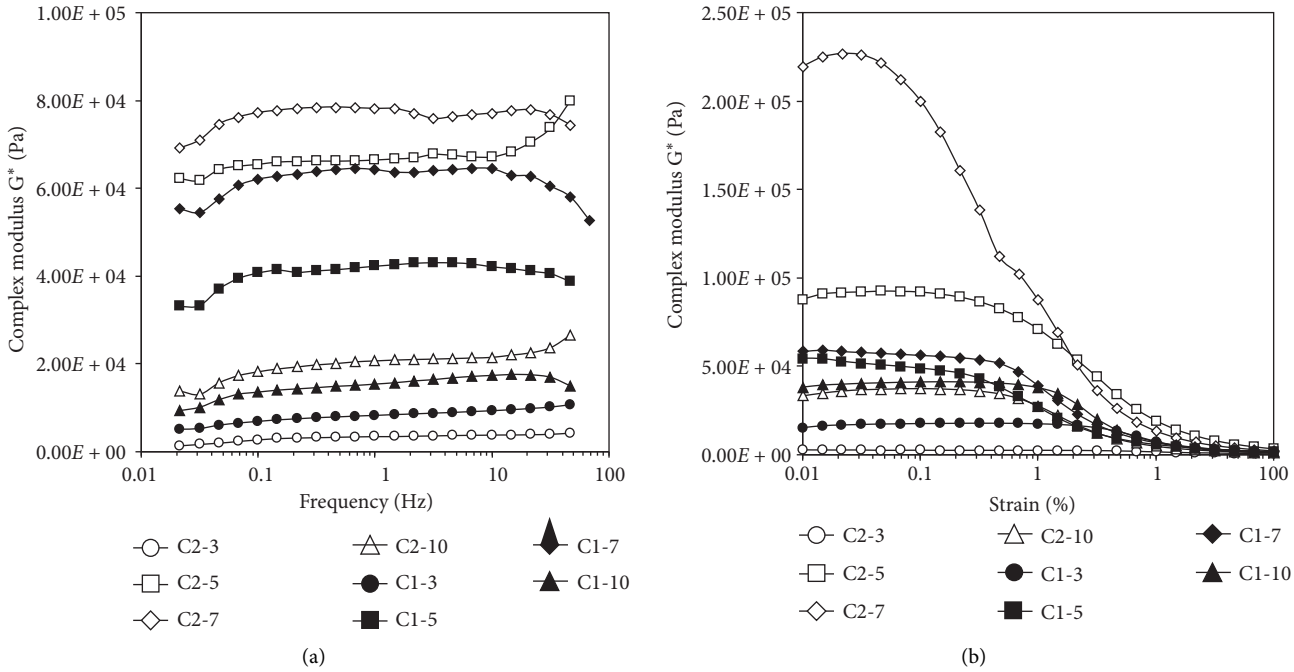

Figure 12: Complex modulus of the chitin hydrogels containing various LiCl concentrations as a function of (a) frequency from 0.01 to 100 Hz and (b) strain from 0.01 to 100%.

C1 and C2 chitin hydrogels (Figure 12(a)). For C1 hydrogel, the G^* values were increased from 6.9 to 62 kPa when the LiCl concentration in DMAc solution was enhanced from 3 to 7% at 0.1 Hz. Changing the chitin concentration to 2%, the G^* values were enhanced as 75 kPa for C2-7, meaning the higher chitin concentration caused the tighter structure of hydrogel. Similar result was observed in the case of 5% LiCl as 40 kPa for C1-5 and 62 kPa for C2-5. As expected, the G^* of the hydrogels prepared at 10% LiCl content was low as 14 kPa and 18 kPa for C1 and C2 samples. It could be observed that the G^* seemed to be constant when the frequency changed. It was due to the relaxation property of the hydrogel material. From Figure 12(b), the values of G^* as a function of strain from 0.01 to 100% were shown. As seen, the G^* of the C1 and C2 hydrogels attributed to the dose dependence of LiCl contents in DMAc solution. For example, when the LiCl amounts increased, the G^* of the C1-3 and C1-7 enhanced from 17.4 kPa to 55.7 kPa at 0.1% of strain. When the chitin concentration was changed as 2%, the C2-7 was obtained as the higher value of G^* than those of C2-5 at a lower strain. However, at a higher strain more than 1%, the G^* value of the C2-7 was significantly decreased because the strain decomposed the hydrogel network. The G^* value was decreased from 10.6 kPa to 4.6 kPa for C2-5 and C2-7 at 10% of strain. Hence, C2-5 exhibited the more stable property than C2-7 at a higher strain. As expected, the complex modulus was lower as 41 kPa for C1-10 and 27.3 kPa for C2-10 due to the reduction of the polymer interaction as the aggregation of chitin segment in the polymer structure of the related hydrogels [10].

4. Conclusion

This is the first paper to describe about the effect of LiCl concentrations on the formation of chitin hydrogel by using the phase inversion process. The chitin chemically extracted from the crab shells waste had the α-form, and the chitin hydrogels prepared at various LiCl concentrations in the DMAc solution expressed different aggregation segments at 3, 5, 7, and 10% LiCl. The chitin solutions prepared with 3% of LiCl showed the low viscosity and the viscous-liked behavior of the obtained chitin hydrogels. The shear viscosity of the chitin solution increased with the higher addition of coagulation water, concluding that the LiCl content could delay the coagulation in the presence of water, resulting in the tight hydrogel which could be obtained. The viscoelasticity of the chitin solution confirmed the stronger entanglement network at a higher LiCl content in DMAc solution due to the formation of the macrocation $[DMAc\text{-}LiCl\text{-}DMAc\text{-}Li]^+$. This ion complex acted as a cross-linker to chitin molecules leading the aggregation of chitin segment in the solution. As the LiCl concentration in DMAc solution increased from 3 to 7%, the mechanical strength and complex modulus of the hydrogel were gradually enhanced. However, the resultant hydrogels prepared at 10% LiCl exhibited the softer structure with low mechanical properties due to the aggregated chitin segments on the hydrogel surface. Moreover, increasing the chitin concentration in the solution showed the enhancement in the mechanical and viscoelasticity of the hydrogels due to the intensification of chain entanglement which was confirmed by the AFM images.

Data Availability

The data used to support the findings of this study are included in the article.

Disclosure

This paper has been presented in a Ph.D. graduation thesis under protection of Nagaoka University of Technology-Chitin Hydrogels prepared with various lithium chloride/*N*,*N*-dimethylacetamide solutions by water vapor-induced phase inversion.

Conflicts of Interest

The authors declare that they have no conflicts of interest.

Authors' Contributions

Khoa Dang Nguyen and Takaomi Kobayashi conceptualized the study. Khoa Dang Nguyen and Takaomi Kobayashi planned the methodology. Khoa Dang Nguyen performed formal analysis and investigation. Khoa Dang Nguyen wrote the original draft presentation. Khoa Dang Nguyen and Takaomi Kobayashi reviewed and edited the manuscript. Takaomi Kobayashi managed the resources. Takaomi Kobayashi supervised the study.

Acknowledgments

The authors would like to thank Asst. Prof. Siriporn Taokaew from Department of Materials Science and Technology, Nagaoka University of Technology, for her support and discussion.

References

[1] A. Boonmahitthisud, L. Nakajima, K. D. Nguyen, and T. Kobayashi, "Composite effect of silica nanoparticle on the mechanical properties of cellulose-based hydrogels derived from cottonseed hulls," *Journal of Applied Polymer Science*, vol. 134, no. 10, 2017.

[2] L. P. R. María, A. G. S. Joaquín, G. Alborno, and J. P. Claudio, "Chitin hydrogel reinforced with TiO_2 nanoparticles as an arsenic sorbent," *Chemical Engineering Journal*, vol. 285, pp. 581–587, 2016.

[3] M. Liu, Y. Zhang, J. Li, and C. Zhou, "Chitin-natural clay nanotubes hybrid hydrogel," *International Journal of Biological Macromolecules*, vol. 58, pp. 23–30, 2013.

[4] D. N. Khoa, T. C. T. Truong, and T. Kobayashi, "Chitin-halloysite nanoclay hydrogel composite adsorbent to aqueous heavy metal ions," *Journal of Applied Polymer Science*, vol. 135, p. 47207, 2018.

[5] E. M. Ahmed, "Hydrogel: preparation, characterization, and applications: a review," *Journal of Advanced Research*, vol. 6, no. 2, pp. 105–121, 2015.

[6] S. Yerang, L. Hyunji, W. L. Jae, and Y. L. Kuen, "Hyaluronate-alginate hybrid hydrogels prepared with various linkers for chondrocyte encapsulation," *Carbohydrate Polymers*, vol. 218, pp. 1–7, 2019.

[7] S. Koki, T. Kohei, T. Yusei, Y. Kazuya, and K. Junichi, "Fabrication of cationic chitin nanofiber/alginate composite materials," *International Journal of Biological Macromolecules*, vol. 91, pp. 724–729, 2016.

[8] O. Z. Ahmadi F, S. M. Samani, and Z. Amoozgar, "Chitosan based hydrogels: characteristics and pharmaceutical applications," *Research in Pharmaceutical Sciences*, vol. 10, no. 1, pp. 1–16, 2015.

[9] F. C. Suk, N. B. R. Ain, C. P. Suh, and S. Lihan, "Antimicrobial starch-citrate hydrogel for potential applications as drug delivery carriers," *Journal of Drug Delivery Science and Technology*, vol. 54, Article ID 101239, 2019.

[10] N. Kazuki and K. Takaomi, "Cytocompatible cellulose hydrogels containing trace lignin," *Materials Science and Engineering C*, vol. 64, pp. 269–277, 2016.

[11] N. Kazuki, I. Shinya, and K. Takaomi, "Biocompatibility evaluation of cellulose hydrogel film regenerated from sugar cane bagasse waste and its in vivo behavior in mice," *Industrial & Engineering Chemistry Research*, vol. 55, pp. 30–37, 2015.

[12] L. L. Shu, K. Joseph, and Y. Fang, "Hydrogels from biopolymer hybrid for biomedical, food, and functional food applications," *Polymers*, vol. 4, no. 4, pp. 997–1011, 2012.

[13] E. Khor, H. Wu, L. Y. Lim, and C. M. Guo, "Chitin-methacrylate: preparation, characterization and hydrogel formation," *Materials*, vol. 4, no. 10, pp. 1728–1746, 2011.

[14] L. T. C. Karla, S. S. Satoshi, T. Motohiro, and T. Kobayashi, "Fibroblast compatibility on scaffold hydrogels prepared from agave tequilana weber bagasse for tissue regeneration," *Industrial & Engineering Chemistry Research*, vol. 52, pp. 11607–11613, 2013.

[15] H. Jiang and T. Kobayashi, "Ultrasound stimulated release of gallic acid from chitin hydrogel matrix," *Materials Science and Engineering: C*, vol. 75, pp. 478–486, 2017.

[16] H. Tang, L. Zhang, L. Hu, and L. Zhang, "Application of chitin hydrogels for seed germination, seedling growth of rape seed," *Journal of Plant Growth Regulation*, vol. 33, no. 2, pp. 195–201, 2014.

[17] K. Naksone and T. Kobayashi, "Effect of pre-treatment of sugarcane bagasse on the cellulose solution and application for the cellulose hydrogel films," *Polymers for Advanced Technologies*, vol. 27, pp. 973–980, 2016.

[18] K. L. T. Carrillo, K. Nakasone, S. Sugita, M. Tagaya, and T. Kobayashi, "Effects of sodium hypochlorite on Agave tequilana Weber bagasse fibers used to elaborate cyto and biocompatible hydrogel films," *Materials Science and Engineering: C*, vol. 42, pp. 808–815, 2014.

[19] S. Taokaew, M. Ofuchi, and T. Kobayashi, "Size distribution and characteristics of chitin microgels prepared via emulsified reverse-micelles," *Materials*, vol. 12, no. 7, p. 1160, 2019.

[20] A. Striegel, "Theory and applications of DMAC/LICl in the analysis of polysaccharides," *Carbohydrate Polymers*, vol. 34, no. 4, pp. 267–274, 1997.

[21] A. C. E. Bianchi, G. Conio, and E. Marsano, "Self-assembly of chitin via a gelation process," *Molecular Crystals and Liquid Crystals Letters*, vol. 7, no. 4, pp. 111–116, 1990.

[22] M. Terbojevich, C. Carraro, A. Cosani, and E. Marsano, "Solution studies of the chitin-lithium chloride-N,N-dimethylacetamide system," *Carbohydrate Research*, vol. 180, no. 1, pp. 73–86, 1988.

[23] K. Sum Chow, E. Khor, and A. Chwee Aun Wan, "Porous chitin matrices for tissue engineering: fabrication and in vitro cytotoxic assessment," *Journal of Polymer Research*, vol. 8, no. 1, pp. 27–35, 2001.

[24] M. Poirier and G. Charlet, "Chitin fractionation and characterization in N,N -dimethylacetamide/lithium chloride

solvent system," *Carbohydrate Polymers*, vol. 50, no. 4, pp. 363–370, 2002.

[25] E. Yilmaz and M. Bengisu, "Preparation and characterization of physical gels and beads from chitin solutions," *Carbohydrate Polymers*, vol. 54, no. 4, pp. 479–488, 2003.

[26] B. Chen, K. Sun, and K. Zhang, "Rheological properties of chitin/lithium chloride, N,N-dimethyl acetamide solutions," *Carbohydrate Polymers*, vol. 58, no. 1, pp. 65–69, 2004.

[27] H. Imen, Ö. Fatih, and J. M. Regenstein, "Industrial applications of crustacean by-products (chitin, chitosan, and chitooligosaccharides): a review," *Trends in Food Science & Technology*, vol. 48, pp. 40–50, 2016.

[28] S. Hajji, I. Younes, O. Ghorbel-Bellaaj et al., "Structural differences between chitin and chitosan extracted from three different marine sources," *International Journal of Biological Macromolecules*, vol. 65, pp. 298–306, 2014.

[29] N. Amri, D. Ghemati, N. Bouguettaya, and D. Aliouche, "Swelling kinetics and rheological behavior of chitosan-PVA/montmorillonite hybrid polymers," *Periodica Polytechnica Chemical Engineering*, vol. 63, no. 1, pp. 179–189, 2019.

[30] S. K. Kundu, M. Yoshida, and M. Shibayama, "Effect of salt content on the rheological properties of hydrogel based on oligomeric electrolyte," *The Journal of Physical Chemistry B*, vol. 114, no. 4, pp. 1541–1547, 2010.

[31] O. P. Gbenebor, S. O. Adeosun, G. I. Lawal, S. Jun, and S. A. Olaleye, "Acetylation, crystalline and morphological properties of structural polysaccharide from shrimp exoskeleton," *Engineering Science and Technology, an International Journal*, vol. 20, no. 3, pp. 1155–1165, 2017.

[32] O. P. Gbenebor, S. O. Adeosun, G. I. Lawal, and S. Jun, "Role of $CaCO_3$ in the physicochemical properties of crustacean-sourced structural polysaccharides," *Materials Chemistry and Physics*, vol. 184, pp. 203–209, 2016.

[33] P. G. Oluwashina, I. A. Emmanuel, and O. A. Samson, "Thermal, structural and acetylation behavior of snail and periwinkle shells chitin," *Progress in Biomaterials*, vol. 6, pp. 97–111, 2017.

[34] L. Tinggou, L. Bin, Z. Xiaodong et al., "Effect of freezing on the condensed state structure of chitin in alkaline solution," *Carbohydrate Polymers*, vol. 82, pp. 753–760, 2010.

[35] C. L. de Vasconcelos, P. M. Bezerril, M. R. Pereira, M. F. Ginani, and J. L. C. Fonseca, "Viscosity-temperature behavior of chitin solutions using lithium chloride/DMA as solvent," *Carbohydrate Research*, vol. 346, no. 5, pp. 614–618, 2011.